Ultrasonic characterization of the Crystallization behavior of Poly(ethylene terephthalate)

Zhao, Lijuan; Sun, Zhigang; Tatibouet, Jacques; Guo, Shaoyun

Publisher's version / la version de l'éditeur:
Journal of Applied Polymer Science, 114, 5, pp. 2731-2739, 2009

Web page / page Web
http://dx.doi.org/10.1002/app.30668
http://nparc.cisti-icist.nrc-cnrc.gc.ca/npsi/ctrl?action=rtdoc&an=10831264&lang=en
http://nparc.cisti-icist.nrc-cnrc.gc.ca/npsi/ctrl?action=rtdoc&an=10831264&lang=fr

Ultrasonic Characterization of the Crystallization Behavior Of Poly(Ethylene Terephthalate)

Lijuan Zhao[1,2], Zhigang Sun[2], Jacques Tatibouët[2], and Shaoyun Guo[1*]

1. The State Key Laboratory of Polymer Materials Engineering, Polymer Research Institute of Sichuan University, Chengdu 610065, China
2. Industrial Materials Institute, National Research Council Canada, 75 de Mortagne Blvd. Boucherville, Quebec, Canada J4B 6Y4

Abstract

Based on the previous observations that the ultrasonic signals are sensitive to the crystallization of polymers (Tatibouet, J.; Piché, L. Polymer 1991, 32, 3147), we have expanded our efforts to study the detail relationship between the ultrasonic signals and crystallization process in the present work. The nonisothermal and isothermal crystallization of virgin poly(ethylene terephthalate) (PET) and PET samples after degradation were studied by using a specially designed pressure-volume-temperature (PVT) device, with which an ultrasonic detector was combined. The results showed that the evolution of the ultrasonic signals not only can be used to probe the crystallization process, but also can qualitatively characterize crystallization rate, crystallinity, crystallite size and amorphous. DSC measurement was used to verify such results. Ultrasonic

* Correspondence author. Fax: 86-28-8540-5886; nic7702@scu.edu.cn (S.Guo)

signals could be as a complementary tool to polymer chain movement and well be applied to characterize the crystallization behavior. Furthermore, the ultrasonic measurement has the potential use to characterize crystallization of products in-line during processing（i.e., injection molding, micromoulding）.

Keywords: ultrasonic; DSC; crystallization; PET

Introduction

Semi-crystalline polymer has complex structures of crystallite and amorphous regions. It is known that polymer crystallites have significant effects on product properties, such as brittleness, strength, deformation temperature, solvent endurance and penetrability. Being able to measure the crystallization behavior and control the crystallization process is important not only for process development, but also for quality control of production. Polymer crystallization involves many aspects, such as crystallization kinetics (including the formation of nuclei and their subsequent growth), crystallite size and shape, crystallinity and crystallite microstructures. But a single measurement method is often insufficient to describe the polymer crystallization process. Differential scanning calorimetry (DSC) is the most widely used technique for studying polymer crystallization.[1,2] Also available are other techniques such as dilatometry,[3] density measurement,[4] infrared (IR) spectroscopy,[5] X-rays diffraction,[6] light scattering[7] and optical microscopy.[8] However, some of the above-mentioned techniques can not be implemented to perform or simulate the real processes. Temperature and pressure sensors

are widely employed in-line to control the polymer processing. However, it is difficult to measure the details of crystallization (i.e., crystallization temperature, crystallinity, crystallization rate), and the feedback information from them is far away sufficient for many of our purposes. But they are still good measurements to help in controlling crystallization process. In the past decades, the fluorescent,[9] visible optical detectors[10] and laser[11] have been used in adopting the investigation of in line polymer processing, but transparent slit is needed to support these techniques.

Ultrasonic technique is an excellent tool for in-line, real-time, non-invasion and non-destructive in polymer characterization. It has been more and more widely used to diagnose polymer processing and characterize polymer properties. Many researches have found that acoustical properties (ultrasonic velocity and attenuation) can characterize polymer's physical properties, including the correlation between ultrasonic parameters with density,[12] relaxation and transition,[13, 14] elastic modulus,[15] the morphology of polymer blends [16] and the orientation of polymer chain in injection molding [17]. In particularly, it is attractive to many researchers to investigate in line ultrasonic applications in recent decades. Nishiwaki,[18] et al. at Tokyo University of Agriculture and Technology, one of the pioneering teams in this area, introduced the application of in-line ultrasonic monitoring for polymer processes in 1985. They reported that the flight time of ultrasonic waves through plastics decreases as the plastics cools down and eventually solidifies. The amplitude variation of the ultrasonic waves reflecting back from the mold and plastics interface could detect the air gap in the interface. Brown,[19] et al. at University

of Bradford, UK, developed an ultrasonic transit time measuring instrument for off-line and in-line polymer process diagnosis. They reported a strong interaction between transit time, melt pressure and temperature, and verified that ultrasound provided sensitive indications of melt process and material properties. Researches conducted at IMI/NRC in this area started in 1990. Gendron,[20] et al. investigated an in-line ultrasonic technique for detecting filler concentration during extrusion. They found that increasing the filler concentration caused the attenuation to increase and ultrasonic velocity to decrease.

By combining ultrasonic testing with conventional pressure-volume-temperature (PVT) device, a measurement system was set up in our group, which named as ultrasonic PVT or UPVT with U, P, V, and T standing for respectively ultrasonic, pressure, specific volume and temperature. UPVT as a laboratory tool has been applied to predict polymer dynamic behavior by simulating polymer processing conditions and to monitor the polymer crystallization kinetic.[21-24] By using UPVT and by measuring the ultrasonic velocity and attenuation in the polymer sample, Tatibouët and Piché[22] were able to determine the melting, chain relaxation and glass transition temperatures of the sample as a function of pressure. Reignier and Tatibouët [24] also studied the effects of dissolved CO_2 molecules in the crystallization kinetics of poly(lactide) by UPVT, and the results showed that crystallization rate was found to significantly increase with a moderate addition of CO_2.

As an important engineering polymer, Poly(ethylene terephthalate) (PET) is widely used in the forms of fibers, sheet and film, whose properties are partly dependent on the

degree and quality of crystallization. Many factors could affect PET crystallization behavior, such as crystallization temperature, degradation, molecular weight, additives and molecular chain orientations.[25, 26] In the literature, the crystallization of PET was well characterized, and the data gave us a good reference at good qualitative conclusions.[27, 28]

In the present work, the crystallization behavior of PET was studied by using the UPVT through comparing virgin and degraded PET samples. The purpose is to see how sensitive the ultrasonic approach would be in measuring crystallization and whether the UPVT can well distinguish the crystallization behavior for the polymer with different structures. DSC measurement was used to verify the UPVT results.

Experimental

PET pellets (9921), supplied by Eastman Chemical, were dried in vacuum at 60 $^{\circ}C$ over 12 hours and then used in the experiments. In order to use ultrasound to understand the crystallization behavior of virgin and degraded PET, four samples with different degree of degradation were prepared using internal mixer on purpose. These four PET samples were prepared (Brabender mixer PL2000) by kneading 60 grams for 20 minutes, and the processing conditions is listed in Table 1. Roller blades were used as mixing elements. The torque values and temperatures were recorded by a computer.

Figure 1 shows a schematic of UPVT system. The design was described in details previously.[21] Characterization of materials is based on the propagation of small-amplitude diagnostic ultrasonic waves and their propagation characteristics including velocity, attenuation and frequency dispersion of the waves in the materials. Ultrasonic waves are

generated from one ultrasonic transducer (UT), passing consecutively through one steel delay line buffer rod, the sample and another steel buffer rod, then received by the other UT. The polymer sample is confined between two steel rods. The thickness of samples is controlled by the displacement of the upper buffer rod. The position is continuously measured with an LVDT displacement transducer and controlled with an accuracy of 1μm. The sample thickness is then used for calculating specific volume V and density ρ ($\rho \equiv 1/V$) of the material. The heating/cooling system controls sample temperatures from -100 to 400 $°C$ with heating/cooling rates varying from 50 to 0.015 $°C/\min$ with stability accuracy of ± 0.1 $°C$ in isothermal conditions. A clamping pressure of up to 100 MPa can be applied and the accuracy is ± 0.02 MPa. The whole system is computer-controlled and all data concerning the thickness of the specimen, temperature, pressure and ultrasonic signals are collected every 10 s. The operating frequency of the ultrasonic transducers is 2.25 MHz. Here, the measurement accuracy of velocity is ± 0.5 m/s.

Both nonisothermal and isothermal crystallization kinetics of 3-4 grams of PET samples were investigated by using the UPVT system. In all the tests, sample were first heated up to 280 $°C$ at a heating rate of 30 $°C/\min$ and then kept at 280 $°C$ for 5 minutes to eliminate the thermal history incurred during sample preparation. Afterwards, samples were cooled down to 30 $°C$ at a cooling rate of 2 $°C/\min$ for a nonisothermal crystallization investigation. According to the velocity and attenuation changes in nonisothermal crystallization, the temperature of crystallization onset could be obtained.

Then, they were also cooled down to set temperatures (i.e., 225, 230, 237 $^{\circ}C$ for virgin PET, 230 $^{\circ}C$ for degraded PET, which are higher than the temperature of crystallization onset) at a cooling rate of 50 $^{\circ}C/\min$ for an isothermal crystallization investigation. Because the weight and thickness of samples are much more than in DSC measurement, the cooling rate in ultrasonic testing should be much slower in order to keep samples cooling uniformly.

A Perkin-Elmer differential scanning calorimetry (DSC-7) was operated to determine the crystallization behavior of samples under a nitrogen flow of $20\,cm^3/\min$. Calibration for the temperature was carried out using a pure Indium prior sample tests to ensure accuracy and reliability of the measurement. A sample with a weight of 8-10 mg was heated to 280 $^{\circ}C$ at a heating rate of 30 $^{\circ}C/\min$ and then kept at 280 $^{\circ}C$ for 5 minutes to erase the thermal history. Then it was cooled down to 50 $^{\circ}C$ at a cooling rate of 10 $^{\circ}C/\min$ for nonisothermal crystallization analysis. PET samples were also cooled down to a set temperature (i.e., 205, 225, 230 $^{\circ}C$ for virgin PET, 205, 217, 225 $^{\circ}C$ for PET1) at a cooling rate of 50 $^{\circ}C/\min$ and maintained at the set temperature for isothermal crystallization analysis for one hour, followed by temperature increase to 280 $^{\circ}C$ at the heating rate of 10 $^{\circ}C/\min$ for enthalpy measurement.

Results and discussion

Degraded degree of PET samples

In order to use ultrasound to understand the crystallization behavior of virgin and degraded PET, four samples with different degree of degradation were prepared as testing

samples using internal mixer on purpose.

As it is well known, viscosity is taken to characterize degradation in torque rheometer. The following relationship is used to convert torque value into viscosity. [29, 30]

$$\eta = \frac{\bar{\tau}}{\bar{\dot{\gamma}}} = \frac{C_2 K}{C_1 N} \qquad (1)$$

where η is the viscosity, $\bar{\tau}$ and $\bar{\dot{\gamma}}$ the mean shear stress and mean shear rate, C_1 and C_2 constants that depend primarily on the dimensions of the torque rheometer, K the measured torque, N the motor speed (rpm). Because of comparing qualitatively, C_1 and C_2 can be regarded as constants. The value of K/N, which can be defined as rpm torque (K'), has the same trend as viscosity, and it is used to denote the degree of degradation.

Figure 2 is the torque rheometer data of PET tested on Brebander mixer, which was measured at various seting temperatures and motor speeds. It is evident that there is a high initial rpm torque (K') during fusion and follows a gradual decrease in K' because of completely melting and then degradation. The curves also show that the melt time of PET1 is slower than PET2 and PET3, and the thermal mechanical degradation is also later and weaker due to lower temperture and motor speed. Furthermore, the K' values of PET2 are a little higher than PET3. From the curve 1, 2 and 3, we can conclude the sequence of degradation degree from low to high is PET1,PET2 and PET3 originated from hydrolysis and chain scission.

Nonisothernal crystallization

Nonisothermal crystallization of virgin and degraded PET samples was examined in

details by using the UPVT system coupled with volumetric measurement shown in Figure 1. Figure 3 displays typical evolution behavior of attenuation coefficient α_L, propagation velocity v_L of longitudinal ultrasonic waves and specific volume $V_{specific}$ in virgin PET with decreasing temperature. The experiment was carried out at the cooling rate of 2 $°C/\min$ from $280\,°C$ to $30\,°C$ under constant pressure of 100 bars. The period from A to B in the figure is the process of nonisothermal crystallization, with location A representing the onset temperature (T_{onset}) of the crystallization, and location B for the completion temperature (T_{end}) of the crystallization. v_L also exhibits a steep increase during the same period, and so does α_L. $V_{specific}$ presents an abrupt change at location A as soon as the crystallization begins. As it is shown in figure 3, there is a local maximum of α_L between A and B, which indicates the completion of primary crystallization, where the acoustic attenuation reaches a maximum due to strong scattering of ultrasonic waves by dispersed spherulites. With further decrease of temperature, the sample enters crystallite perfection or secondary crystallization, leading to reducing interface between crystallite and amorphous phases. Consequently, this phenomenon results in less scattering loss of acoustic energy or smaller acoustic attenuation coefficient appearing at around 195 °C.

As the temperature continues to decrease, v_L becomes larger and larger whereas $V_{specific}$ continues to drop because of polymer solidification. In the meantime, α_L exhibits another strong maximum at location C around $150\,°C$, showing the relaxation region under this frequency.[22] As we know, the location of the measured relaxation region

depends on the frequency.[31] When mechanically measured at low frequencies (~1 Hz), the α-relaxation is about $75\,^{\circ}C$. Here, as mentioned before, the frequency used in ultrasonic waves is 2.25 MHz and the relaxation temperature shift greatly. The above observations demonstrate that ultrasound can be an effective tool for the analysis of polymer crystallization.

The evolutions of v_L versus temperature decrease involved in a crystallization process are displayed in Figure 4 for all samples, and the T_{onset} and T_{end} temperatures are listed in table 2. As can be seen, the virgin PET begins to crystallize at the lowest temperature, as indicated with arrow 0 in the figure. However, PET3 starts to crystallize at the highest temperature as indicated with arrow 3 in the figure. Its crystallization also ends earlier than the others. The PET2 sample starts at a higher temperature than PET1, as indicated by arrows 2 and 1 in the figure. During the crystallization period, the ultrasound velocity v_L increases linearly with temperature for all samples, with a slope as listed in table 2. Since the same cooling rate was used for all samples, the values of slopes can be used to compare nonisothermal crystallization growth rates among the samples. The value of slopes suggest that the virgin PET has the slowest crystallization rate compared to the degraded ones and PET2 has a faster crystallization rate than PET1 and PET3. Although PET3 starts to crystallize earlier, its crystallization rate is slower than that of PET1 and PET2. The difference in the crystallization rates between the virgin PET and degraded PET comes from the competition between the formation of nuclei and their subsequent growth during crystallization process. Nuclei in molten polymer can be

formed through two mechanisms: heterogeneous and homogeneous nucleation. Heterogeneous nucleation is due to the presence of a second phase. Impurities or residues of unmelted polymer already existed in the bulk, which serves as nuclei during the crystallization process. Homogeneous nucleation occurs in the absence of a second phase, whose nuclei are formed from polymer bulk chains when temperature is cooled down to be able to make polymer chains "frozen". Then other polymer chains start to grow upon the "frozen" chains which act as polymer nuclei. The whole crystallization process is a continuous competition between nucleation and diffusive transport of polymer chains to nuclei. The overall crystallization rate depends on the number of available nuclei and the rate of transport of molecules. Although virgin PET contains a certain heterogeneity density, mostly derived from catalytic resident, the nucleation density of PET1, PET2 and PET3 should be more than virgin one due to some degraded materials and other impurities. Thus degraded samples crystallize earlier than that of the virgin PET. Because of degradation, the polymer chains in degraded PET are shorter than virgin one, and the rate of transport of molecules in degraded PET is faster than virgin one. Therefore, degraded PET has faster the overall crystallization rate. Nevertheless, for PET1, PET2 and PET3, competitive results between nucleation density and crystal growth are that PET1 has a faster non-isothermal crystallization rate than PET3, but a slower rate than PET2. As it is known, nucleation and crystal growth are relating to chain mobility and entanglements. Virgin PET and degraded PET have various morphology and structures. Thus, different molecular weight and morphology of samples result in various

crystallization behavior,[7,32] which is described clearly by the data of v_L versus T.

During the crystallization process of a semi-crystalline material, as in the case of PET, the $V_{specific}$ changes as a result of increase in crystallinity. This makes $V_{specific}$ measurement be an accepted technique for the study of a crystallization process [33]. Figure 5 shows the variations of $V_{specific}$ versus temperature decrease for the virgin and degraded PET samples. For all samples, $V_{specific}$ reduces with decreasing temperature. During the period of crystallization, all samples experience a sudden reduction in specific volume. However, the virgin PET has the slowest reduction rate comparing to degraded PET samples. The slopes of $V_{specific}$ curves for PET1 and PET2 are a little sharper than that of PET3.

Variation of α_L with temperature decrease is presented in Figure 6 for four samples studied. The T_{onset} of each sample is also seen clearly, as in the case of $V_{specific}$ and v_L measurements. However, α_L has a distinct feature compared to virgin and degraded PET. The virgin PET has the pronounced peak at around 195 °C which is not seen in the other samples. When radius of the nuclei is equal to the wavelength, the wave scattering will be largest, and the local maximum of attenuation will occur. However, in our experiment, crystal particle size is smaller than wavelength (wavelength is about 1 mm). The local maximum of attenuation comes out when the spheres start to percolate and come into contact, whereupon it decreases as the medium becomes more homogeneous[34, 35]. Because virgin PET crystallizes slowly and crystal size should be bigger than that of other samples, [36, 37] the acoustic attenuation coefficient is larger in the case of the virgin

PET due to more scattering loss of the acoustic energy at the interface of larger crystallite spherulites. However, more nucleation centers, fast crystallization rate and dense nuclei in degraded PET make the boundaries between crystallites contact once crystallite growth. Thus this local maximum is not observed in the case of degraded PET. The dependence of the signal of α_L with T and crystallization morphology is complex and generally crystallization kinetics cannot be investigated by using only the absolute attenuation as a parameter. As mentioned in Figure 3, the region around $150\,°C$ is identified as the relaxation. In this region, the main relaxation is attributed to amorphous phase and is sensitive to crystallinity.[22, 38] Acoustic attenuation in the relaxation region can qualitatively characterize the crystallinity. Since larger acoustic attenuation in this region is the consequence of larger amorphous content, the larger acoustic attenuation coefficient of the virgin PET means less the crystallinity compared with the degraded PET samples. In the relaxation region, the attenuation curve of PET1 almost superposes that of PET2, indicating that PET1 and PET2 have similar crystallinity, which is however, less than that of PET3.

Nonisothermal crystallization behavior of the virgin and degraded PET was also examined using DSC with the results shown in Figure 7, and the T_{onset} and T_{end} temperatures are listed in table2. Comparing the T_{onset} of the degraded samples, which are indicated with arrows 1, 2, and 3 for PET1, PET2, and PET3 samples, respectively, it is obviously that PET3 crystallizes earlier than PET2 while PET2 crystallizes earlier than PET1. This is consistent with the ultrasonic results. However, it is difficult to detect the

heat flow resulted from the crystallization of the virgin PET even at a low cooling rate of 2 $°C/\min$ because of slow crystallization rate and low crystallinity. Interestingly, the crystallization behavior of the same virgin PET was detected easily by ultrasound. The exothermic enthalpy values of PET1, PET2 and PET3 samples are 39.0 J/g, 41.9 J/g and 44.7 J/g, respectively. This means PET3 has the largest crystallinity whereas PET1 has the smallest. The crystallinity of PET2 is only slightly above that of PET1. This is consistent with the qualitative results provided by the ultrasonic attenuation measurement.

The above-discussed results demonstrate that the ultrasound can be a good and sensitive investigation tool for the analysis and understanding of nonisothermal crystallization processes, and it can give additional information comparing with $V_{specific}$ and DSC measurement.

Isothermal tests

Tests were performed to see if ultrasound UPVT can well investigate isothermal crystallization kinetics for different degraded PET under different measurement conditions as well. The test temperatures were kept above the T_{onset} of the nonisothermal crystallization processes discussed earlier. Figures 8, 9 and 10 show the variations with time of v_L, $V_{specific}$ and α_L during isothermal crystallization kinetics of the virgin PET carried out at 225, 230, and $237\,°C$, respectively. Among these three tests, v_L measured at 225 $°C$ in Figure 8 shows the steepest slope at the beginning of the process before

reaching a plateau. This means that at lower temperature, the crystallization takes place faster and completes sooner. The variations of $V_{specific}$ displayed in Figure 9 show similar trends to v_L but in an inversed direction. Figure 10 shows the evolutions of α_L in the same processes. Depending on the testing temperature, α_L presents a maximum at different time. As discussed earlier, the peak of α_L indicates the completion of the primary crystallization. In the test carried out at $225\,°C$, the peak value reaches earlier than the other two tests, which indicates that the sample crystallizes faster at this temperature than at the higher temperatures. The initial slope of α_L at $225\ °C$ is also steeper compared with those at 230 and $237\,°C$. Since variation in α_L during crystallization process is mainly attributed to the scattering loss of ultrasonic energy by crystallites, the rate at which α_L increase can be directly related to the speed at which crystallites are forming and growing. The relationship is as follows $\alpha_{scattering} \propto N \cdot \Delta K^2 \cdot r^3$, where N is number of scattering particles, $\Delta K = (K_1 - K_2)$ moduli difference and r scattering radius. So, if N (nuclei) is constant at given T, $d\alpha/dt$ is proportional to $(r^2 \cdot dr/dt)$. Therefore, the steeper slope seen in the α_L curve at $225\ °C$ indicates that the sample crystallizes faster than at the higher temperatures. The comparisons among the three peak locations show clearly that the crystallization time is strongly reduced when the test temperature is decreased.

In Figure 11 and 12, the isothermal crystallization behavior at the same temperature of $230\,°C$ is compared for the virgin and degraded PET. Similar to the nonisothermal processes presented earlier, the changes of v_L (Figure 11) and $V_{specific}$ (Figure 12) are

faster for the degraded PET than for the virgin PET, implying faster isothermal crystallization rates of the degraded PET. Moreover, PET3 crystallizes faster than the others. However, there is no significant difference between PET1 and PET2 in the isothermal crystallization rate.

The isothermal crystallizations of the virgin PET and PET1 have also been investigated by using DSC. Because virgin PET is difficult to crystallize, the melt peak is very weak under higher temperature, for example 230 $°C$. Thus lower temperatures are set for virgin PET. By contrast, degraded PET (PET1 as example) can crystallize in higher temperature. In the tests, the samples were cooled down from molten state to the set temperature above T_{onset} of the nonisothermal crystallization processes discussed earlier. Then the sample was kept at this set temperature for one hour for polymer isothermal crystallization. After this, the sample was heated up to 280 $°C$ and the heat flow was recorded. Figure 13 shows the recorded heating curves, and table 2 lists the melting temperatures. For the virgin PET, it is also difficult to detect the heat flow for the sample which is isothermally crystallized at 225 $°C$. This is because the crystallization temperature of 225 $°C$ is too high for the sample to crystallize effectively. At lower temperatures of 217 $°C$ and 205 $°C$, crystallization is taking place in more efficient manner, and higher crystallinity is reached. For the PET1 samples, melting peaks are detected even for the PET1 sample isothermally crystallized at 230 $°C$. This means it is easier for PET1 to crystallize than for the virgin PET due to different nucleation mechanism and chain mobility involved. As can be seen in the figure, the sample which

crystallizes at lower temperature (for example PET1 at 205 °C) starts to melt at lower temperature (as indicated with arrow f) than those crystallize at high temperatures (for example PET1 at 230 °C , which the onset melting temperature is indicated with arrow d). The difference in the onset melting temperatures and the multiple melting endothermic are attributed to the presence of different distributions of lamella thickness.[39]

Conclusions

The ultrasonic results of crystallization kinetics of a virgin and degraded PET samples were compared with those obtained by using DSC measurements. The comparisons have demonstrated that ultrasound was also able to detect the crystallization behavior which was detectable by the DSC measurements. The acoustic parameters are sensitive to polymer crystallization behavior and it can be as a complementary method to be used to validate other measurement results. One distinctive advantage of ultrasound compared with DSC measurement is that the ultrasonic technology presented in this paper can be implementable in-line or on-line for real-time monitoring of a crystallization process during production (for example during the cooling stage of an injection molding process).

Acknowledgment

L.Zhao acknowledges the financial support of Chinese Scholarship Council (CSC), China.

References

1. Cayuela, D.; Gacén, J.; Tzvetkova, M.; Gacén, I.; Amrein, M. Polym Testing 2008, 27, 667.

2. Zhang, F.; Zhou, L.; Xiong, Y. Q.; Liu, G.. P.; Xu, W. J. J Appl Polym Sci 2009, 111, 2930.
3. Kojima, M.; Magill, J. H. Polymer 1985, 26, 1971.
4. Mitra, D.; Misra, A. J. App. Polym. Sci 1988, 36, 387.
5. Jang, J.; Sim, K. Polym Testing 1998, 17, 507.
6. Knaepen, W.; Detavernier, C.; Van, M. R. L.; Jordan, S. J.; Lavoie, C. Thin Solid Films 2008, 516, 4946.
7. Fanegas, N.; Gómez, M. A.; Marco, C.; Jiménez, I.; Ellis, G.. Polymer 2007, 26, 144.
8. Aju Joseph, T.; Koch, S.; Seidler, S.; Thomas, K. J Appl Polym Sci 2008, 109, 1714.
9. Bur, A. J.; Vangel, M. G.; Roth, S. Appl Spectrosc 2002, 56, 174.
10. Melo, T. J. A.; Canevarolo, S. V. Polym Eng Sci 2002, 42, 170.
11. Francis, P. S.; Martin, S.; Bryant,G.;. Megen, W. V.; Wilksch, P. A. Rev Sci Instrum 2002, 73, 3878.
12. Nidal, H. Int. J. Adv Manuf Technol 2004, 24, 661.
13. Parthun, M.; Johari, G.. P. J Chem Phys 1995, 102, 6301.
14. Sahnoune, A.; Massines, F.; Piché, L. J Polym Sci Part B. Polym Phys 1996, 34, 341.
15. Lavrentyev, A. I.; Rokhlin, S. I. Ultrasonics 2001, 39, 211.
16. Verdier, C. ; Piau, M . J Phys D: Appl Phys 1996, 29, 1454.
17. Edwards, R.; Thomas, C. Polym Eng Sci 2001, 41,1644.
18. Nishiwaki, N.; Hori, S.; Tsutsumi, M. JSPE 1986, 52, 507.
19. Brown, E.C.; Collins, T.L.D.; Dawason, A.J.; Olley, P.; Coates, P.D. J Rein Pla Comp

1999, 18, 331.

20. Gendron, R.; Daigneault, L.; Taibouet, J.; Dumoulin, M. Adv Polym Tech 1996, 15, 111.

21. Piché, L.; Massines, F.; Hamel, A.; Hubert, S.; Neron, C. U.S. Patent 4754645.

22. Tatibouët, J.; Piché, L. Polymer 1991, 32, 3147.

23. Tatibouët, J.; Gendron, R.; Haider, L. Polym Testing 2004, 23,125.

24. Reignier, J.; Tatibouët, J.; Gendron, R. RAPRA Conference Proceedings on Blowing Agents and Foaming Processes, Frankfurt, Germany, 2007.

25. Cavalcanti, F. N.; Teófilo, E. T.; Rabello, M. S.; Silva, S. M. L. Polym Eng Sci 2007, 47, 2155.

26. Karagiannidis, P. G.; Stergiou, A. C.; Karayannidis, G.. P. Europ Polym J 2008, 44, 1475.

27. Müller, A. J.; Feijoo, J. L.; Alvarez, M. E.; Febles, A. C. Polym Eng Sci 1987, 27, 796 .

28. Stoeffler, K.; Lafleur, P. G.. J Polym Degd Stab 2008, 93, 1332.

29. Goodrich, J. E.; Porter, R. S. Polym Eng Sci 1967, 7, 45.

30. Melik, D. H. Schechtman, L. A. Polym Eng Sci 1995,35,1975.

31. Shi, W.; Fang, C. S.; Pan, Q. W.; Sun, X.; Gua, Q. T.; Xu, D.; Yu, J. Z. React Funct Polym 2000, 44, 177.

32. Van, A. F.; Van, K. D. J Polym Sci part B: Polym Phys 1972, 10, 2423.

33. Ito, H.; Tsutsumi, Y.; Minagawa, K.; Takimoto, J.; Iwakura, K.; Koyama, K. Colloid

Polym Sci 1995, 273, 811.

34. Granham, I. S.; Piché, L.; Levesque, D. Phys Rev B, 1991, 43, 10769.

35. Liegey, F. ; Tatibouët, J.; Derdouri, A. ANTEC 2004.

36. Wu, T. M.; Lin,Y. W. J Polym Sci Part B: Polym Phys 2004, 42, 4255.

37. Chung, J. W.; Son, S-B.; Chun, S-W.; Kang, T-J.; Kwak, S-Y. Polym Degd Stab 2008, 93, 252.

38. Benatmane, A.; Tatibouët, J.; Vigier, G..; Bourgin, P. Actes colloque I.D. Matériaux, Paris, 1989, 402.

39. Lu, X. F.; Hay, J. N. Polymer 2001, 42, 9423.

Figure 1. The schematic of ultrasonic measurement device.

Figure 2 Torque rheometer data of PET at various set temperatures and motor speeds.

Figure 3. Simultaneous measurements of v_L, α_L (at $f = 2.25$ MHz), and $V_{specific}$ of a virgin PET. Cooling from 280 $°C$ to 30 $°C$ at a cooling rate of 2 $°C/\min$. A constant pressure of 10 MPa.

Figure 4. Variations of v_L versus temperature decrease for virgin and three degraded PET samples, provided by our device at a cooling rate of $2\,°C/\min$. A constant pressure of 10 MPa.

Figure 5. Variations of $V_{specific}$ versus temperature decrease for virgin and three degraded PET samples.

Figure 6. Variations of α_L versus temperature decrease for virgin and three degraded PET samples.

Figure 7. DSC patterns of nonisothermal crystallization for the virgin and degraded samples.

Figure 8. Isothermal crystallization diagrams for the virgin PET at three temperatures for v_L. A constant pressure of 10 MPa.

Figure 9. Isothermal crystallization diagrams for the virgin PET at three temperatures for $V_{specific}$.

Figure 10. Isothermal crystallization diagrams for the virgin PET at three temperatures for α_L.

Figure 11. Isothermal crystallization diagrams for v_L for the virgin and degraded PET at

230 $^{\circ}C$.

Figure 12. Isothermal crystallization diagrams for $V_{specific}$ for the virgin and degraded PET at 230 $^{\circ}C$.

Figure 13. DSC heating curves at a heating rate of 10 $^{\circ}C/\min$ for the virgin PET and PET1 under various isothermal crystallization temperatures.

Table 1 Processing conditions and abbreviations for PET samples.

Table 2 The parameters during nonisothermal and isothermal crystallization processing.

Table 1

Sample codes	Processing Temperature ($°C$)	Kneading speed (rpm)
Virgin PET	--	--
PET1	260	40
PET2	260	70
PET3	270	70

Table 2

Parameters			Virgin PET	PET1	PET2	PET3
UPVT nonisothermal crystallization	T_{onset} $°C$ ($\pm 0.5°C$)		212.4	220.1	223.9	228.0
	T_{end} $°C$ ($\pm 0.5°C$)		188.7	211.5	212.8	215.6
	Growth rates $(m/s)/°C$		-10.7	-20.2	-24.0	-15.3
DSC nonisothermal crystallization	T_{onset} $°C$ ($\pm 0.5°C$)		-----	194.3	196.0	200.4
	T_{end} $°C$ ($\pm 0.5°C$)		----	157.3	165.6	172.5
DSC isothermal crystallization	$T_{melting}$ $°C$ ($\pm 0.5°C$)	230	----	248.2	------	
		225	----	----		
		217	243.6	245.2		
		205	241.2	238.4		

Figure 1

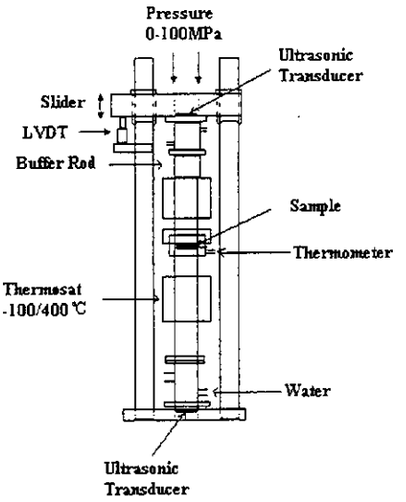
Pressure
0-100MPa
Ultrasonic
Transducer
Slider
LVDT
Buffer Rod
Sample
Thermometer
Thermosat
-100/400℃
Water
Ultrasonic
Transducer

Figure2

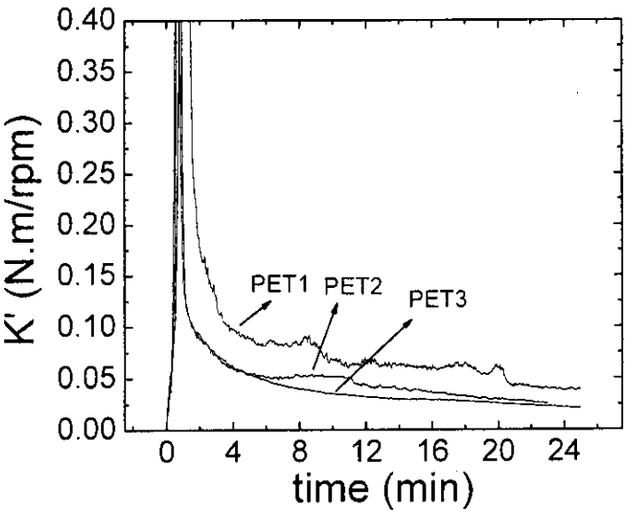
0.40
0.35
0.30
0.25
0.20
0.15
0.10
0.05
0.00
K' (N.m/rpm)
PET1
PET2
PET3
0
4
8
12
16
20
24
time (min)

Figure 3

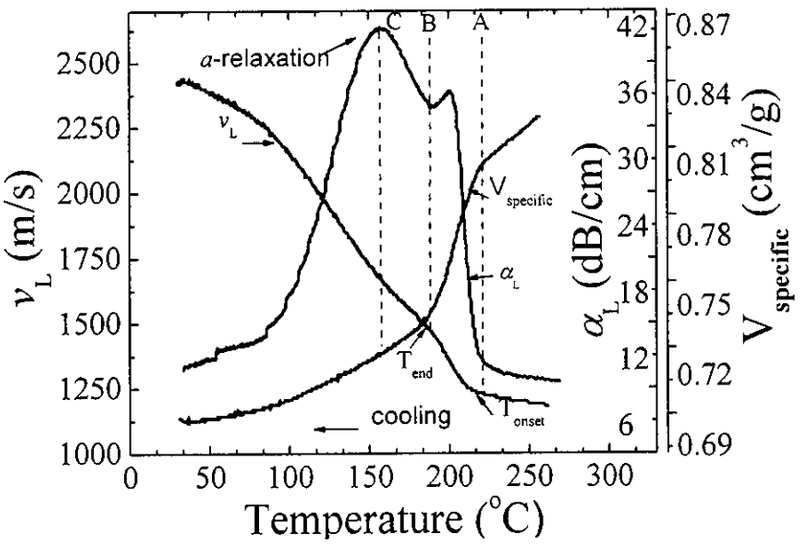
C
B
A
a-relaxation
v_L
$V_{specific}$
α_L
T_{end}
T_{onset}
cooling
v_L (m/s)
α_L (dB/cm)
$V_{specific}$ (cm^3/g)
Temperature (°C)
2500
2250
2000
1750
1500
1250
1000
0
50
100
150
200
250
300
42
36
30
24
18
12
6
0.87
0.84
0.81
0.78
0.75
0.72
0.69

Figure 4

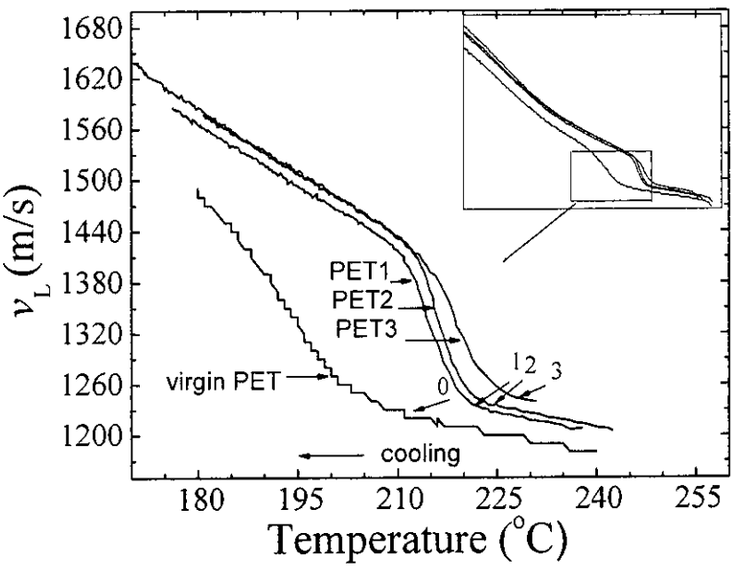
1680
1620
1560
1500
1440
1380
1320
1260
1200
v_L (m/s)
PET1
PET2
PET3
virgin PET
0
1 2 3
cooling
180
195
210
225
240
255
Temperature (°C)

Figure 5

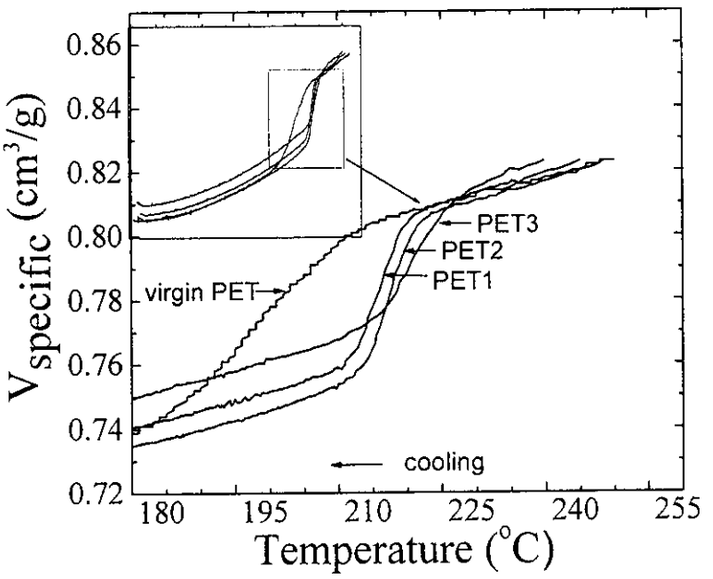
0.86
0.84
0.82
0.80
0.78
0.76
0.74
0.72
$V_{specific}$ (cm^3/g)
PET3
PET2
PET1
virgin PET
cooling
180
195
210
225
240
255
Temperature (^oC)

Figure 6

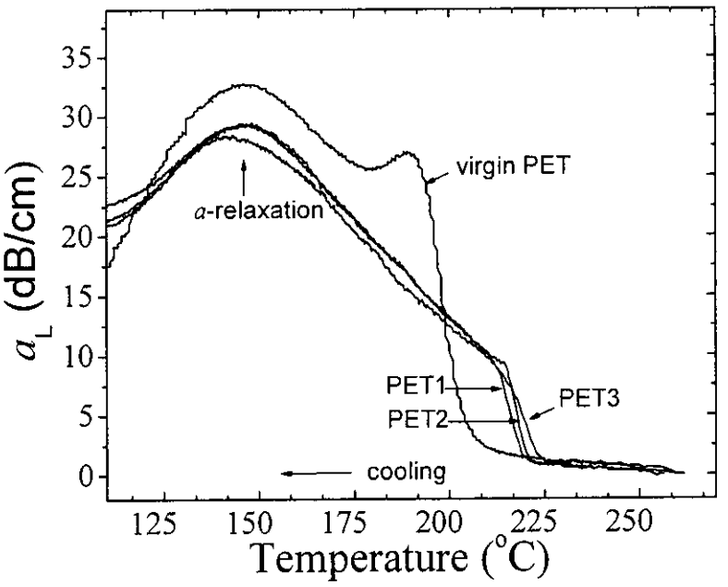
35
30
25
20
15
10
5
0
a_L (dB/cm)
125
150
175
200
225
250
Temperature (°C)
virgin PET
a-relaxation
PET1
PET2
PET3
cooling

Figure 7

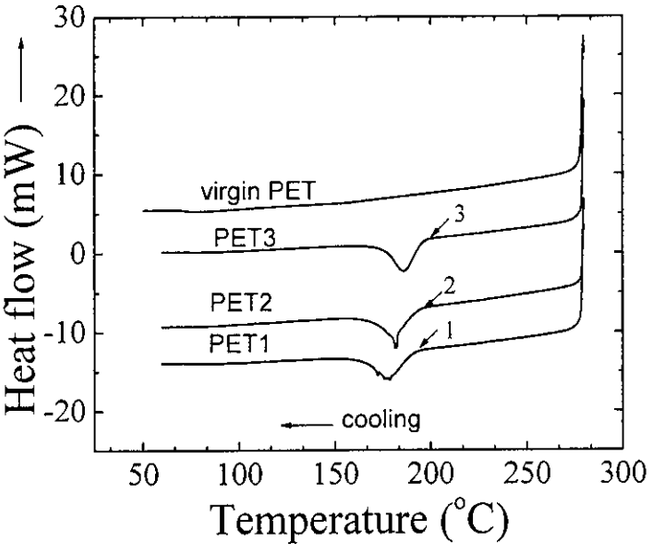
Heat flow (mW)
30
20
10
0
-10
-20
virgin PET
PET3
PET2
PET1
3
2
1
cooling
50
100
150
200
250
300
Temperature (°C)

Figure 8

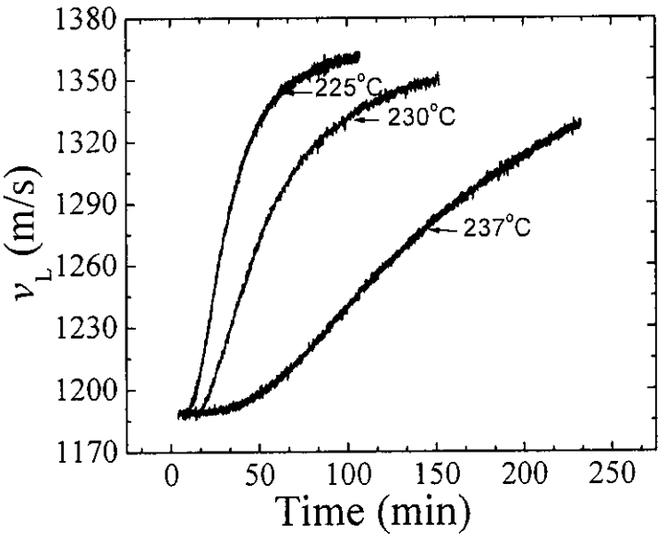
1380
1350
1320
1290
1260
1230
1200
1170
v_L (m/s)
225°C
230°C
237°C
0
50
100
150
200
250
Time (min)

Figure 9

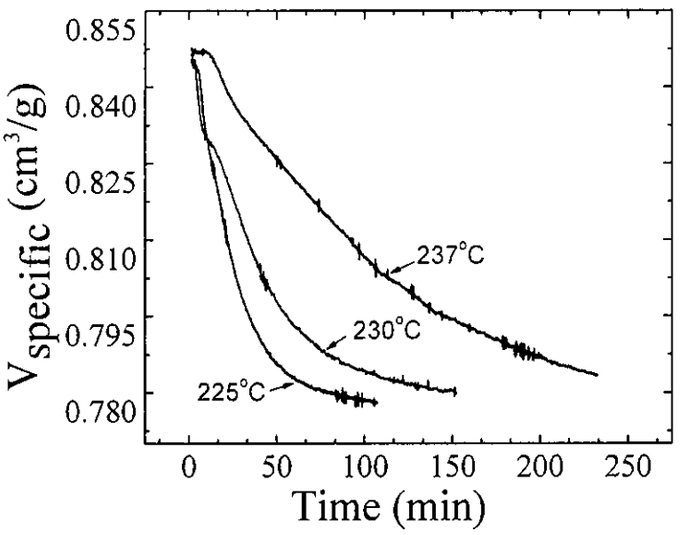
0.855
0.840
0.825
0.810
0.795
0.780
$V_{specific}$ (cm^3/g)
237°C
230°C
225°C
0
50
100
150
200
250
Time (min)

Figure 10

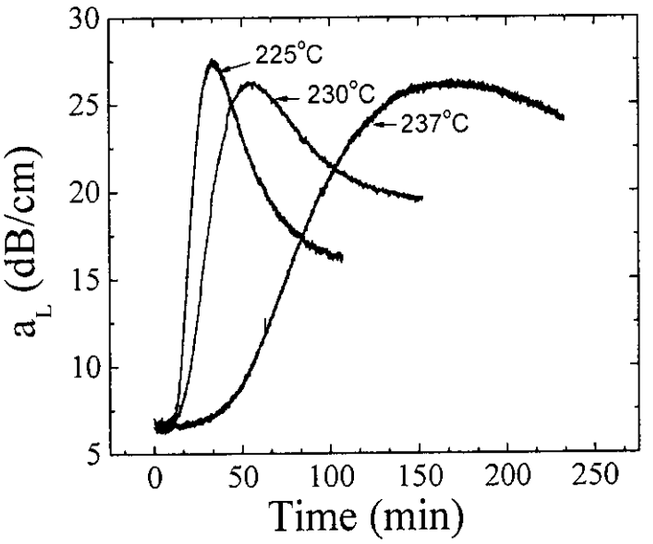
30
25
20
15
10
5
a_L (dB/cm)
225°C
230°C
237°C
0
50
100
150
200
250
Time (min)

Figure 11

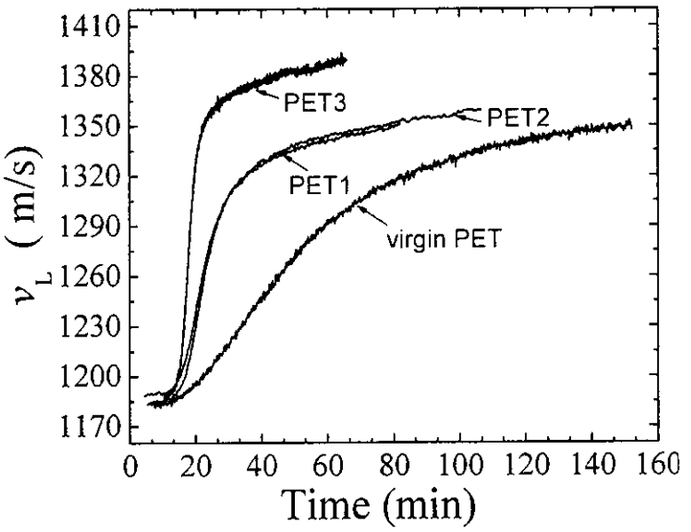
1410
1380
1350
1320
1290
1260
1230
1200
1170
v_L (m/s)
0
20
40
60
80
100
120
140
160
Time (min)
PET3
PET2
PET1
virgin PET

Figure 12

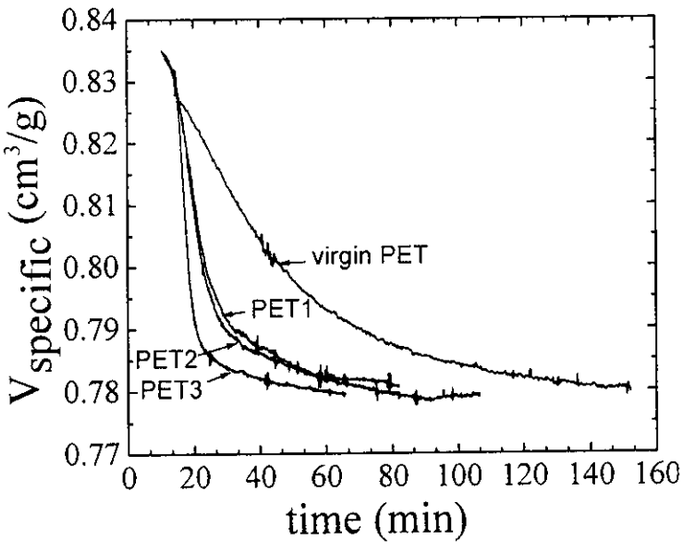
0.84
0.83
0.82
0.81
0.80
0.79
0.78
0.77
V specific (cm3/g)
0
20
40
60
80
100
120
140
160
time (min)
virgin PET
PET1
PET2
PET3

Figure 13

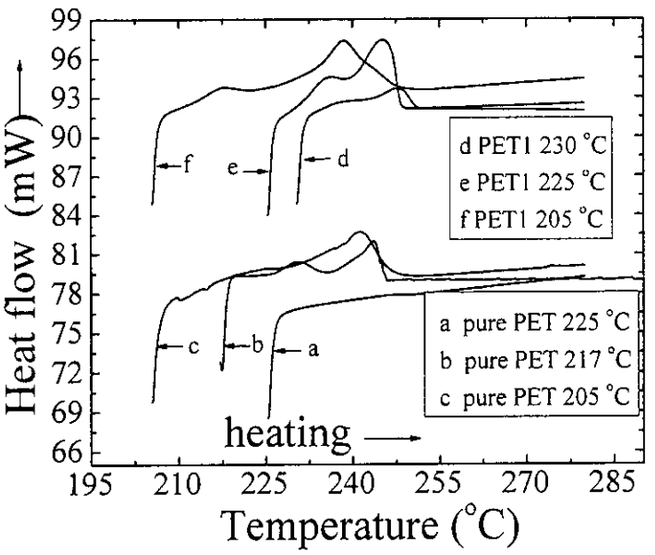
Heat flow (mW)
99
96
93
90
87
84
81
78
75
72
69
66
195
210
225
240
255
270
285
Temperature (°C)
f
e
d
c
b
a
d PET1 230 °C
e PET1 225 °C
f PET1 205 °C
a pure PET 225 °C
b pure PET 217 °C
c pure PET 205 °C
heating